The Structure and Physical Properties of a Novel Three-Dimensional Zeolite-Like Nanoporous Architecture Formed by Two Different Polymeric Layers: $[Eu_2(btc)(H_2btc)(H_2O)]\cdot 4H_2O$

Chuan-De Wu,[a] Can-Zhong Lu,*[a] Wen-Bin Yang,[a] Shao-Fang Lu,[a] Hong-Hui Zhuang,[a] and Jin-Shun Huang[a]

Keywords: Hydrothermal synthesis / Nanostructures / Materials science / Europium / Organic-inorganic hybrid composites

The open framework of $[Eu_2(btc)(H_2btc)(H_2O)]\cdot 4H_2O$ (**1**), prepared by hydrothermal reaction of $EuCl_3$ with 1,2,4,5-benzenetetracarboxylic anhydride in acidified aqueous solution, is built up from two types of polymeric layers with $[EuO_6(H_2O)]_n$ units as tethers, resulting in nanoporous channels that host water molecules through complex hydrogen bonding. Crystallographic data for **1**: monoclinic, $P2_1/n$, with a = 10.7562(2) Å, b = 7.2075(2) Å, c = 17.2180(5) Å, β = 97.072(2)° and Z = 2. A study of the temperature dependence of the magnetic susceptibility data reveals that the paramagnetic behavior of **1** is mainly due to the effective spin-orbital coupling between the ground and exited states through the Zeeman perturbation; the magnetic interaction between europium(III) centers is very weak. A study of the electronic properties demonstrates that compound **1** is a semiconductor. A TGA analysis between 30 and 600 °C for **1** suggests that when the lattice water molecules are removed from the network, the skeleton of the network still remains stable up to 150 °C; this is also confirmed by XRPD.
(© Wiley-VCH Verlag GmbH, 69451 Weinheim, Germany, 2002)

Introduction

In the past few years, the construction of inorganic coordination networks, especially of zeolite-like microporous materials, has attracted much attention[1−4] not only because of their intriguing architectures, but also because of their promising potential applications.[5−7] The design and synthesis of new frameworks containing large pores that can facilitate the removal/adsorption of guest molecules is a continuing challenge.

We are currently interested in pursuing synthetic strategies that use lanthanide ions as nodes for the construction of three-dimensional microporous frameworks. Such structures are more difficult to control than those of d-block transition metal analogues due to the higher coordination numbers of lanthanide ions and the inherent flexibility of their coordination geometries, which could lead to unprecedented topological architectures. Recent reports have demonstrated that some organic ligands have a dramatic impact on structures, and consequently on their properties, and are therefore very useful for the control of the architectures of coordinated polymers.[8−11] The 1,2,4,5-Benzenetetracarboxylic (pyromellitic) acid (H_4btc) ligand,[12] which has eight (btc) or four (H_2btc) potential donor oxygen atoms, is a rather versatile ligand for the synthesis of polymeric complexes with metal cations.[13] However, examples of H_4btc-bridged metal-organic frameworks that can maintain their structural integrity upon the removal of guest molecules are still rare. In the course of our investigations on the synthesis of btc- and/or H_2btc-bridged f-block lanthanide metal-based materials, we realized that the unique lanthanide nature, the H_4btc ligand and the reaction conditions could work synergistically to produce new 3D porous open frameworks. Here we report the synthesis and crystal structure of $[Eu_2(btc)(H_2btc)(H_2O)]\cdot 4H_2O$ (**1**), as well as some new phenomena observed during the course of investigations of its physical properties.

Results and Discussion

The hydrothermal reaction of an acidified aqueous solution of $EuCl_3$ with 1,2,4,5-benzenetetracarboxylic anhydride gives rise to **1** as colorless crystals. A single crystal X-ray analysis revealed that the three-dimensional microporous framework of compound **1** is built by linking one crystallographically independent nine-coordinate Eu^{III} subunit through its btc and H_2btc ligands. Each nine-coordinated Eu^{III} unit is a distorted tricapped trigonal prism, of which eight oxygen atoms belong to six different carboxylate groups of btc or H_2btc and the other one to a water molec-

---

[a] The State Key Laboratory of Structural Chemistry, Fujian Institute of Research on the Structure of Matter, the Chinese Academy of Sciences,
Fuzhou, Fujian 350002, P. R. China
Fax: (internat.) + 86-0591/371-4946
E-mail: czlu@ms.fjirsm.ac.cn

Supporting information for this article is available on the WWW under http://www.eurjic.com or from the author.

ule, with the $Eu^{III}-O$ bond lengths ranging from 2.353(4) to 2.581(4) Å.

Interestingly, there are two types of coordination modes for the H_4btc ligands in compound **1** (I and II). In mode I, each H_4btc unit acts as a dodecadentate ligand coordinating six europium(III) atoms, that is, each of the four carboxylate groups chelates to one Eu^{III} center, while every two adjacent oxygen atoms of the nearest carboxylate groups coordinate to one more europium(III) atom (Figure 1). In mode II, only two of the four carboxylate groups of an H_4btc ligand coordinate to europium(III) centers and each carboxylate group coordinates to two different Eu^{III}, thus, each ligand coordinates to four europium(III) centers (Figure 2). The H_4btc ligand links europium(III) atoms in very different ways to produce two different infinite network layers. The layers of these two types interlock with each other with a fold of about 60° to form a unique three-dimensional microporous framework with channels (dimensions about 10.331 × 11.201 Å). The zigzag $[EuO_6(H_2O)]_n$ tethers, which are built up from nine-coordinate europium(III) atoms with Eu−Eu distances of about 3.950(1) Å, are bridged by carboxyl oxygen atoms and the carboxylate groups of H_4btc. The channels are filled with eight water molecules per unit cell, which can be replaced by other suitable molecules under certain conditions (Figure 3). Finally, it should also be pointed out that the distances between guest water oxygen atoms are about 2.83(1) Å, while those between the water oxygen atoms and the oxygen atoms of the carboxylate groups range from 2.65(1) to 3.08(1) Å. Additionally, the distances between the oxygen atoms of coordinated water molecules and guest water molecules or carboxylate groups are also within the hydrogen bonding ranges [2.75(1) to 2.97(1) Å], indicating a complex hydrogen bonding network in the packing of compound **1**.

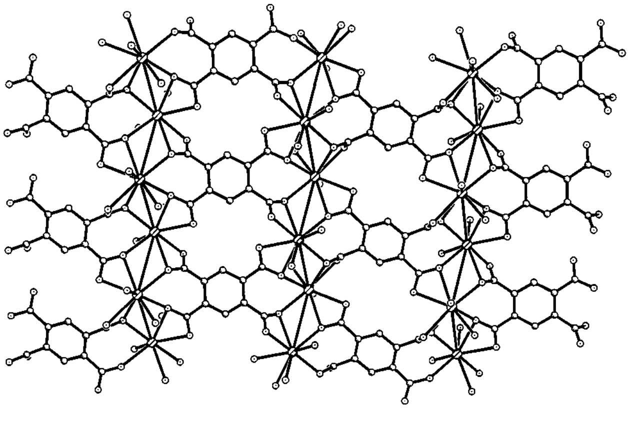

Figure 1. View of an intralamellar structure down the *a* axis for **1**, showing the environments of Eu^{III} atoms and one of the coordination modes for H_4btc

The variation of the molar magnetic susceptibility χ_M was investigated for compound **1** in the temperature range from 5.0 to 300 K in a 10 KG applied field. Figure 4 shows the magnetic behavior of **1** in the form of $\chi_M T$ vs. T and χ_M vs. T plots. At 299.2 K, the $\chi_M T$ value is 1.262 emu·K·mol^{-1} per Eu^{III}, and upon cooling to 5.0 K the $\chi_M T$ values decrease gradually to 0.0288 emu·K·mol^{-1}, indicating the presence of a strong paramagnetic coupling in compound **1**.

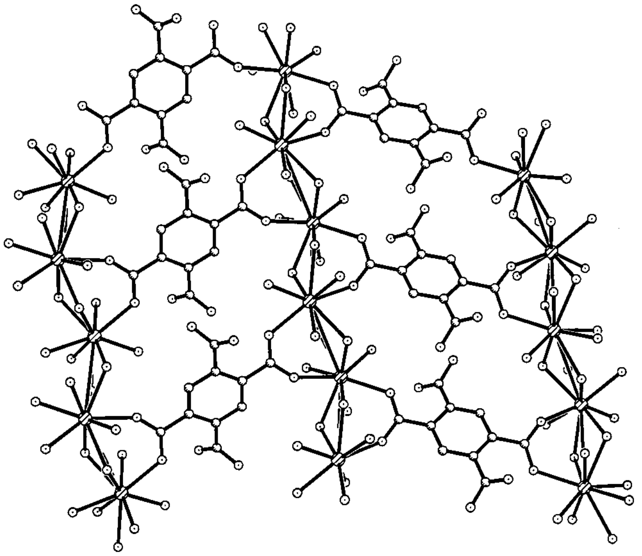

Figure 2. Side view of another intralamellar structure of **1**, showing the environments of the Eu^{III} atoms and the second coordination mode for H_4btc

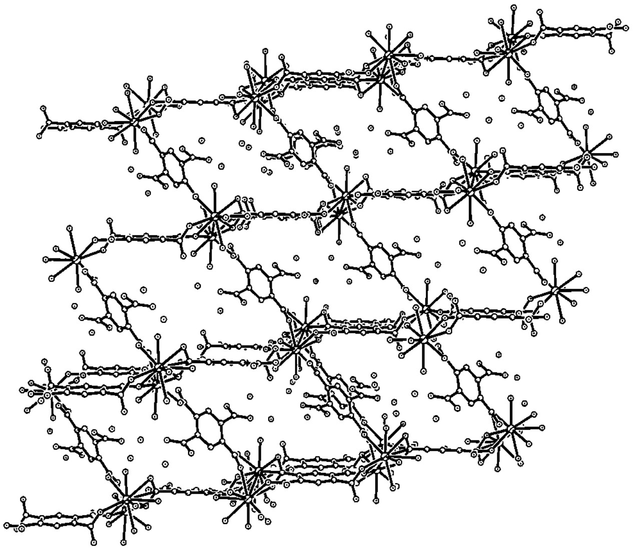

Figure 3. View down the *b* axis showing the channels that are occupied by water molecules in **1**

In contrast with transition metal compounds, the magnetic properties of rare earth metal compounds, even of mononuclear species, have not yet been fully understood. According to the literature,[14] the effect of the crystal field is not easily calculated, while the angular momentum often plays a key role in the magnetic susceptibilities of rare earth metal compounds. For the trivalent europium ion, the ^7F ground term is split by the spin orbit coupling into seven

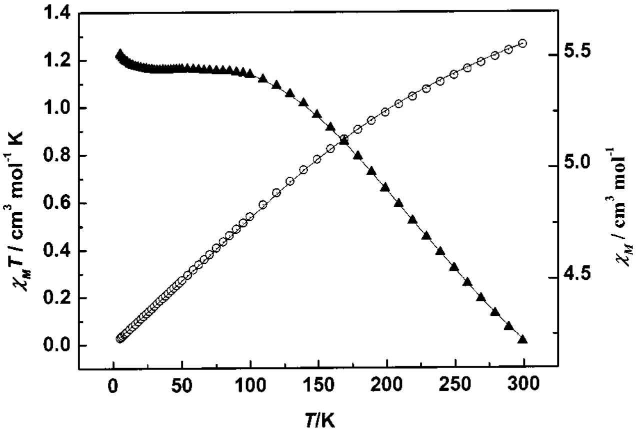

Figure 4. The $\chi_M T$ vs. T and χ_M vs. T plots for compound **1**

states, ^7F_J ($J = 0, 1, 2, ... 6$). Thus, the removal of the $2J + 1$ degeneracy of the ground state at zero field and the thermal population of the free-ion exited states must be considered in this case for Eu^{III}; these factors obviously cause the deviation from normal Curie–Weiss behavior. Based upon the above discussion, the magnetic susceptibility data were quantitatively analyzed using Equation (1):

$$\chi_M = N\beta^2/3k(T - \theta)x[24 + (27x/2 - 3/2)e^{-x} + (135x/2 - 5/2)e^{-3x} + (189x - 7/2)e^{-6x} + (405x - 9/2)e^{-10x} + (1485x/2 - 11/2)e^{15x} + (2457x/2 - 13/2)e^{-21x}]/[1 + 3e^{-x} + 5e^{-3x} + 7e^{-6x} + 9e^{-10x} + 11e^{-15x} + 13e^{-21x}] \quad \text{with } x = \lambda/kT \tag{1}$$

In this case, λ is the spin-orbit coupling parameter between ground and exited states through the Zeeman perturbation, while θ is the Curie–Weiss temperature. A least-squares fitting of all experimental data leads to λ and θ values of 393.99 cm^{-1} and 0.897 K with an agreement factor R of 2.0×10^{-5} ($R = \Sigma[(\chi_M)_{\text{obs}} - (\chi_M)_{\text{calcd}}]^2/\Sigma[(\chi_M)^2_{\text{obs}}]$). These results demonstrate that all of the europium(III) ions are well isolated from each other in the magnetic molecular field, even if the Eu–Eu distance is rather short [3.950(1) Å]. The paramagnetic behavior is mainly due to the spin-orbital coupling and weak ferromagnetic interactions between Eu^{III} centers transferred through oxygen atoms and the ligands.

Determination of the conductivity (powder sample from ground crystals) gives a value of 3.01×10^{-7} Scm^{-1} at 303 K for **1**, and it increases as the temperature rises, indicating that **1** is a semiconductor. This semiconducting behavior of **1**, which demonstrates the existence of either Eu–Eu or Eu–L–Eu interactions, is probably due to the unique structural feature whereby the arrays of Eu^{III} atoms are coordinated by bridging oxygen atoms, and to the short Eu–Eu distance [3.950(1) Å].

The overall neutral three-dimensional framework of **1** shows clearly the presence of large channels, which are occupied by water molecules. These guest molecules can be removed to generate nanoporous solids with retention of the framework skeleton. The thermogravimetric analysis (TGA) data graph shows a four-stage weight loss for compound **1**. The first stage, which occurs from 30–190 °C, is attributed to the loss of the four crystal water molecules per formula unit. The observed weight loss (7.3%) is in agreement with the calculated value (7.0%). The second stage occurs between 190–230 °C, with a weight loss corresponding to one aqua ligand per empirical formula (calcd. 2.0%; found 1.7%). The weight of the molecule remains almost unchanged in the third stage (230–410 °C). At 410 °C, the product begins to lose btc and H_2btc ligands and then to decompose.

A sample of **1** was ground and heated at 150 °C for 24 h at 10^{-2} Torr and then an XRPD spectrum was recorded of the remains. The characteristic peaks are almost identical to those of freshly prepared sample of **1**, which suggests that the hybrid organic-inorganic skeleton is retained. This result demonstrates clearly that the unique framework of **1** is rather stable and its application as a nanoporous material is very promising.

Conclusion

In summary, it is well-known that hydrothermal reactions often produce unprecedented complexes with interesting properties.[15] However, to produce novel complexes with desirable properties under mild reaction conditions is still the preferred option for most chemists. The successful isolation of complex **1** is an example of how to carry out hydrothermal reactions at relatively low temperatures (100 °C). Our strategy not only yields a novel architecture, but also allows us to understand more about whether the reactions are controlled by thermodynamic or by kinetic factors. Although the Eu–Eu distance in the $[EuO_6(H_2O)]_n$ chain is rather short [3.950(3) Å], the magnetic study reveals that the paramagnetic behavior of **1** is mainly due to the coupling among the populated free-ion states, which causes the magnetic behavior to deviate from the Curie–Weiss law. This work provides very important evidence that shows that the free-ion approximation is also appropriate for the interpretation of the magnetic properties of polynuclear rare earth metal species, while the contribution from the overlap of the magnetic orbitals can be almost ignored. The semiconducting behavior of **1** demonstrates the existence of metal-metal interactions. Based upon the TGA and XRPD analyses, the structure is rather stable, and this is undoubtedly due to the multidentate ligands forming a rigid framework for **1**. Moreover, from these studies, compound **1** is one of the few compounds that maintains its structural integrity after the removal of guest molecules. We have reasons to believe that it has potential applications for shape-selective reactions[16] or solvent-exchange process,[17] and these are now under investigation.

Experimental Section

Synthesis of 1: The pH of a mixture of $EuCl_3$ (0.68 mmol) (prepared from Eu_2O_3 dissolved in 35% HCl) and 1,2,4,5-benzenetetracarboxylic anhydride (0.22 g, 1.0 mmol) in H_2O (18 mL) was adjusted to 1.22 whilst stirring vigorously and the resulting mixture was then heated at 100 °C for twelve days under autogenous pressure in a sealed 30 mL Teflon-lined stainless steel vessel. Colorless crystals were isolated after the reaction solution was cooled down gradually and washed with water and ethanol. Yield: 0.239 g (76.8%, based on Eu). $C_{20}H_{18}Eu_2O_{22}$ (914.26): calcd. C 26.27, H 1.98; found C 26.19, H 1.96. IR (KBr pellet): $\tilde{\nu}$ = 1878w cm^{-1}, 1659s, 1610s, 1579s, 1554s, 1498s, 1429sh, 1387s, 1336m, 1323m, 1294s, 1269s, 1142w, 1124s, 849m, 933m, 881s, 849m, 835s, 816m, 775m, 754m, 658m, 590s, 521s, 442m. FT-Raman (solid, λ = 1064 nm): $\tilde{\nu}$ = 1677m cm^{-1}, 1633sh, 1594s, 1579s, 1459s, 1440sh, 1419sh, 1390sh, 1278m, 1253m, 1187s, 973s, 898s, 848s, 825m, 794s, 682s, 597w, 489m, 478m, 456m, 399m, 331m, 304w, 250m, 215m, 179m, 165m, 138m, 119m.

X-ray Crystallography: The determination of the unit cell and the data collection for a colorless crystal of compound **1** were performed on a Siemens SMART CCD, and the data were collected using graphite-monochromated Mo-K_α radiation (λ = 0.71073 Å) at 293 K in the range of $2.12 < \theta < 25.05°$. The data set was corrected with the SADABS program.[18] The structure was solved by direct methods and refined by full-matrix least-squares methods, which were performed using the SHELXL-97 software package.[19] All non-hydrogen atoms were refined anisotropically. Crystal data: $C_{20}H_{18}Eu_2O_{22}$, M_r = 914.26, monoclinic, space group $P2_1/n$, a = 10.7562(2), b = 7.2075(2), c = 17.2180(5) Å, β = 97.072(2)°, U = 1324.68(6) Å^3, Z = 2, D_c = 2.292 gcm^{-3}, μ = 4.795 mm^{-1}, $F(000)$ = 880, crystal size = 0.30 × 0.06 × 0.04 mm^3. $R1$ = 0.0289, $wR2$ = 0.0613 and S =1.077 for 1943 reflections with $F_o > 4\sigma(F_o)$ and 216 parameters ($R1$ = 0.0414 and $wR2$ = 0.0681 for all 2316 data). CCDC-160794 contains the supplementary crystallographic data for this paper. These data can be obtained free of charge at www.ccdc.cam.ac.uk/conts/retrieving.html [or from the Cambridge Crystallographic Data Centre, 12, Union Road, Cambridge CB2 1EZ, UK; fax: (internat.) +44-1223/336-033; E-mail: deposit@ccdc.cam.ac.uk].

Acknowledgments

We are grateful to the State Education Ministry, the State Personal Ministry, the National Natural Science Foundation of China (20073048), the NSF of Fujian and the Chinese Academy of Sciences for financial support.

---

[1] W. F. Hölderich, H. van Bekkum, in *Introduction to Zeolite Science and Practice* (*Stud. Surf. Sci. Catal.* **1991**, *58*, 631−727).

[2] S. M. Csicsery, *Zeolites* **1984**, *4*, 202−213.

[3] S. S.-Y. Chui, S. M.-F. Lo, J. P. H. Charmant, A. G. Orpen, L. D. Willians, *Science* **1999**, *283*, 1148−1150.

[4] M. J. Zaworotko, *Angew. Chem.* **2000**, *112*, 3180−3182; *Angew. Chem. Int. Ed.* **2000**, *39*, 3052−3054.

[5] H. Li, M. Eddaoudi, T. L. Groy, O. M. Yaghi, *J. Am. Chem. Soc.* **1998**, *120*, 8571−8572.

[6] C. Janiak, *Angew. Chem.* **1997**, *109*, 1499−1502; *Angew. Chem. Int. Ed. Engl.* **1997**, *36*, 1431−1434.

[7] G. B. Gardner, D. Venkataraman, J. S. Moore, S. Lee, *Nature* **1995**, *374*, 792−795.

[8] M. L. Occelli and H. C. Robson, in *Zeolite Synthesis*, American Chemical Society, Washington DC, **1989**.

[9] C. T. Kresge, M. E. Leonowicz, W. J. Roth, J. C. Vartuli, J. S. Beck, *Nature* **1992**, *359*, 710−712.

[10] L. L. Hench, *Inorganic Biomaterials*, in *Materials Chemistry, an Emerging Discipline*, (Eds.: L. V. Interrante, L. A. Caspar and A. B. Ellis), ACS Ser. 245, **1995**, ch. 21, pp. 523−547.

[11] P. J. Hagrman, D. Hagrman, J. Zubieta, *Angew. Chem.* **1999**, *111*, 2798−2848; *Angew. Chem. Int. Ed.* **1999**, *38*, 2638−2684.

[12] F. Takusagawa, K. Hirotsu, A. Shimada, *Bull. Chem. Soc. Jpn.* **1971**, *44*, 1274−1278.

[13] For several examples, see: [13a] A. Nectoux, H. Abazli, J. Jove, A. Cousson, M. Pages, M. Gasperin, G. Choppin, *J. Less-Common Met.* **1984**, *97*, 1−10. [13b] A. Cousson, B. Stout, F. Nectoux, M. Pages, *J. Less-Common Met.* **1986**, *125*, 111−115. [13c] C. Robl, *Z. Anorg. Allg. Chem.* **1987**, *554*, 79−86. [13d] Y. Xing, Z.-S. Jin, Z.-B. Duan, J.-Z. Ni, *Acta Chim. Sinica* **1987**, *45*, 1044−1047. [13e] O. M. Yaghi, H. Li, T. L. Groy, *Z. Kristallogr.-New Crystal Structures* **1997**, *212*, 457. [13f] B. T. Usubaliev, A. N. Shnulin, Kh. S. Mamedov, *Koord. Khim.* **1982**, *8*, 1532−1538. [13g] C. Robl, S. Hentschel, *Mater. Res. Bull.* **1991**, *26*, 1355−1362. [13h] F. Jaber, F. Charbonnier, R. Faure, *J. Chem. Cryst.* **1997**, *27*, 397−400. [13i] C. Robl, *Mater. Res. Bull.* **1992**, *27*, 99−107. [13j] F. R. Rochon, G. Massarweh, *Inorg. Chim. Acta* **2000**, *304*, 190−198.

[14] [14a] M. Andruh, E. Bakalbasis, O. Kahn, J. C. Trombe, P. Porcher, *Inorg. Chem.* **1993**, *32*, 1616−1622. [14b] E. Bakalbasis, O. Kahn, J. Sainton, J. C. Trombe, J. Gaiy, *J. Chem. Soc., Chem. Commun.* **1991**, 755−756.

[15] [15a] J. Gopalakrishnan, *Chem. Mater.* **1975**, *7*, 1265. [15b] A. Rabenau, *Angew. Chem.* **1985**, *97*, 1017−1031; *Angew. Chem. Int. Ed. Engl.* **1985**, *24*, 1026−1040. [15c] R. A. Ludise, *Chem. Eng. News* **1987**, *65*(40), 30−43. [15d] J. Y. Lu, M. L. Lawandy, J. Li, T. Yuen, C. L. Lin, *Inorg. Chem.* **1999**, *38*, 2695−2704.

[16] M. Hölscher, U. Englert, B. Zibrowins, W. F. Hölderich, *Angew. Chem.* **1994**, *106*, 2552−2554; *Angew. Chem. Int. Ed. Engl.* **1994**, *33*, 2491−2493.

[17] [17a] M. Fujita, O. Sasaki, K. Watanabe, K. Ogura, K. Yamaguchi, *New. J. Chem.* **1998**, *22*, 189. [17b] L. Carlucci, G. Liani, D. M. Proserpio, S. Rizzato, *Angew. Chem.* **2000**, *112*, 1566−1570; *Angew. Chem. Int. Ed.* **2000**, *39*, 1506−1510.

[18] G. M. Sheldrick. SADABS; Siemens Analytical X-ray Instrument Division: Madison, WI, **1995**.

[19] G. M. Sheldrick, Universität Göttingen, Germany, **1997**.

Received September 21, 2001
[I01374]